

Optimal series representations for numerical path integral simulations

Cristian Predescu and J. D. Doll

Department of Chemistry, Brown University, Providence, Rhode Island 02912

(dated: December 31, 2021)

By means of the Ito-Nisio theorem, we introduce and discuss a general approach to series representations of path integrals. We then argue that the optimal basis for both "primitive" and partial averaged approaches is the Wiener sine-Fourier basis. The present analysis also suggests a new approach to improving the convergence of primitive path integral methods. Current work indicates that this new technique, the "reweighted" method, converges as the cube of the number of path variables for "smooth" potentials. The technique is based on a special way of approximating the Brownian bridge which enters the Feynman-Kac formula and it does not require the Gaussian transform of the potential for its implementation.

PACS numbers: 02.70.Ss, 05.30.-d

Keywords: density matrix; path integrals; random series; Monte Carlo

I. INTRODUCTION

Numerical simulations based on the path integral approach have proved highly successful in the calculation of thermodynamic properties for complex, many-body quantum systems (see Refs. 1,2 and the cited bibliography). Mainly the result of Feynman³ and Kac,⁴ the centerpiece of the theory is the fact that the density matrix of a monodimensional system can be written as the expectation value of a suitable functional of a standard Brownian bridge $fB_u^0; 0 \leq u \leq 1$. More precisely, if $fB_u; u \in [0,1]$ is a standard Brownian motion starting at zero, then the Brownian bridge is the stochastic process $fB_u; B_1 = 0$; $0 \leq u \leq 1$ i.e., a Brownian motion conditioned on $B_1 = 0$.⁵ In this paper, we shall reserve the symbol E to denote the expected value (average value) of a certain random variable against the underlying probability measure of the Brownian bridge B_u^0 . For a monodimensional canonical ensemble characterized by the inverse temperature $\beta = 1/(k_B T)$ and made up of identical particles of mass m_0 moving in the potential $V(x)$, the Feynman-Kac density matrix formula reads:^{3,4,6}

$$\frac{\rho_{fp}(x; x^0; \beta)}{\rho_{fp}(x; x^0; \beta)} = E \exp \left[-\frac{\beta}{m_0} \int_0^1 V(x_0(u)) + \frac{1}{2} \dot{x}_0^2(u) du \right]; \quad (1)$$

where $\rho_{fp}(x; x^0; \beta)$ stands for the density matrix of a similar free particle canonical ensemble, while $x_0(u)$ is a shorthand for $x + (x^0 - x)u$.

Current research is focused on the development of accurate, finite-dimensional approximations of the stochastic integrals that appear in Eq. 1 and in related thermodynamic expressions. The importance of Eq. 1 as given here consists of the fact that the Brownian motion, hence the Brownian bridge, are well understood mathematical objects, which can be simulated by a variety of means. The discussion in the present paper is based on the random series technique as a general representation scheme for the Brownian bridge B_u^0 . The approach is particularly interesting, as it is directly related to the "path integral"

concept, and can be justified by means of the Ito-Nisio theorem,⁷ whose statement is presented in Appendix A.

We consider a number of questions related to the random series implementation of the Feynman-Kac formula. The so called primitive³ and partial averaging⁹ techniques, developed initially for the Fourier path integral (FPI) method,⁸ are generalized here for arbitrary series representations. Then, we address the question of whether or not there exists a preferred basis within which to implement the two techniques. We present strong evidence suggesting that the fastest convergent series for each method is the Wiener series on which the Fourier path integral approach is based. Finally, we introduce a new, non-averaging technique called the reweighted FPI method in order to improve the convergence of primitive FPI.

Motivated by the optimality of the Wiener series, we undertake the task of establishing numerically the asymptotic rate of convergence for the three FPI methods: the primitive FPI, the partial averaging FPI (PA-FPI), and the reweighted FPI (RW-FPI). The asymptotic rate of convergence of the primitive FPI was extensively studied^{2,10} and is known to be $O(1/n)$ for sufficiently smooth potentials. However, there are at present no analytical or numerical studies concerning the exact asymptotic behavior of the PA-FPI method. For the particular case of the harmonic oscillator, it is known that the asymptotic rate of convergence is $O(1/n^3)$. (The reader should not mistake the full PA-FPI for the so called gradient corrected PA-FPI, which was shown to converge as fast as $O(1/n^2)$ in Ref. 10 for potentials having continuous second-order derivatives). To cope with the numerical difficulties encountered, we develop a Monte Carlo technique which allows us to study the asymptotic behavior of the PA-FPI and RW-FPI methods, at least for single-well potentials. With its help, we find strong numerical evidence suggesting that the asymptotic rate of convergence for both PA-FPI and RW-FPI approaches is $O(1/n^3)$ for sufficiently smooth potentials. To our knowledge, RW-FPI thus becomes the most rapidly convergent method among those that leave the original potential un-

changed.

The error analysis performed in Appendix E allows us to introduce what we call "accelerated" estimators, which are capable of improving the rate of convergence of any of the aforementioned methods from $O(1/n)$ to $O(1/n^{+1})$ for the first-order correction, and to $O(1/n^{+2})$ for the second-order correction, respectively. Although there is a price paid in the form of an increase in the variance of the respective estimators, the first-order correction appears suitable for general applications.

II. SERIES REPRESENTATIONS OF THE BROWNIAN BRIDGE

The most general series representation of the Brownian bridge is given by the Ito-Nisio theorem, the explicit statement of which is presented in Appendix A. We begin by assuming that we are given $f_k(\cdot)g_{k-1}$, a system of functions on the interval $[0;1]$, which, together with the constant function, $\phi_0(\cdot) = 1$, make up an orthonormal basis in $L^2[0;1]$. If \mathcal{A} is the space of infinite sequences $a = (a_1; a_2; \dots)$ and

$$P[a] = \prod_{k=1}^{\infty} (a_k) \quad (2)$$

is the (unique) probability measure on \mathcal{A} such that the coordinate maps $a \mapsto a_k$ are independent identically distributed variables with distribution probability

$$(a_k \in A) = \frac{1}{2} \int_A e^{-z^2/2} dz \quad (3)$$

then,

$$B_u^0(a) \stackrel{d}{=} \sum_{k=1}^{\infty} a_k \phi_k(u); \quad 0 \leq u \leq 1 \quad (4)$$

i.e., the right-hand side random series is equal in distribution to a standard Brownian bridge. Therefore, the notation $B_u^0(a)$ in (4) is appropriate and allows us to interpret the Brownian bridge as a collection of random functions of argument a , indexed by u .

Using the Ito-Nisio representation of the Brownian bridge, the Feynman-Kac formula (1) takes the form

$$\frac{(x; x^0; \cdot)}{f_p(x; x^0; \cdot)} = \int_0^1 dP[a] \exp \int_0^1 V(x_0(u) + \sum_{k=1}^{\infty} \frac{1}{\sqrt{2}} \sum_{k=1}^{\infty} a_k \phi_k(u) du) \quad (5)$$

To reinforce the formula (5), consider the functions $\frac{1}{\sqrt{2}} \cos(k \cdot) g_{k-1}$, which, together with the constant function, make up a complete orthonormal system of $L^2[0;1]$. Since

$$\int_0^1 \frac{1}{2} \cos(k \cdot) d = \frac{1}{2} \frac{\sin(k \cdot)}{k};$$

the Ito-Nisio theorem implies that

$$B_u^0 \stackrel{d}{=} \sum_{k=1}^{\infty} \frac{1}{\sqrt{2}} \sum_{k=1}^{\infty} a_k \frac{\sin(k \cdot)}{k}; \quad 0 \leq u \leq 1; \quad (6)$$

so that the Feynman-Kac formula (5) becomes

$$\frac{(x; x^0; \cdot)}{f_p(x; x^0; \cdot)} = \int_0^1 dP[a] \exp \int_0^1 V(x_0(u) + \sum_{k=1}^{\infty} \frac{1}{\sqrt{2}} \sum_{k=1}^{\infty} a_k \sin(k \cdot) du) \quad (7)$$

where

$$\frac{1}{k} = \frac{2}{m_0} \frac{1}{k^2};$$

Equation (7), derived here as a special case of the Ito-Nisio theorem, is the so-called Fourier path integral method.⁸ Historically, the sine-Fourier representation was one of the first explicit constructions of the Brownian motion.¹¹ Following the mathematical literature, we shall call it the Wiener construction after the name of its author, even though the original FPI method was deduced using arguments other than those presented here.

The "primitive" series representation method consists of approximating the Brownian bridge by the n -th order partial sum of the series (4). Thus,

$$\frac{f_p^n(x; x^0; \cdot)}{f_p(x; x^0; \cdot)} = \int_0^1 dP[a] \exp \int_0^1 V(x_0(u) + \sum_{k=1}^n \frac{1}{\sqrt{2}} \sum_{k=1}^n a_k \phi_k(u) du) \quad (8)$$

An immediate question arises: What is the best choice of functions $\phi_i(u)$; $i = 1, \dots$, independent of potential, such that (8) has the fastest convergence? Although the phrase "independent of potential" carries ambiguities, in the remainder of this section we shall provide a more precise statement of the problem.

We start with the observation that the Wiener basis is the only basis for which both $\phi_i(u)$, and their primitives $\phi_i(u)$; $i = 1, \dots$ are orthogonal. Indeed, let us notice that by construction, $\phi_i(0) = 0$ for $i = 1$ and that

$$\int_0^1 \phi_i(1) \phi_j(0) d = 0 \quad \text{if } i \neq j$$

by orthogonality and the fact that $\phi_0(\cdot) = 1$. The unique basis, $\phi_i(u)$, for which

$$\begin{aligned} \int_0^1 \phi_i(1) \phi_j(0) d &= 0; \quad \text{if } i \neq j \\ \int_0^1 \phi_i(1) \phi_j(1) d &= \delta_{ij}; \quad \text{if } i, j = 1 \\ \phi_i(0) &= \phi_i(1) = 0; \quad \text{if } i = 1 \end{aligned}$$

is made (up to a multiplication factor) of the eigenfunctions of the Dirichlet problem :

$$\frac{1}{2} \varphi_i(u) = e_{i-1}(u); \quad \varphi_i(0) = \varphi_i(1) = 0;$$

as follows from the associated Dirichlet variational principle and the non-degeneracy of the spectrum of the "particle in a box problem". But that basis is precisely the Wiener basis.

The orthogonality of the primitives, $\varphi_i(u)$, suggests that the Wiener basis is (in a sense that will be made clear below) optimal for the representation of the Brownian bridge. Let us define

$$S_u^n(a) = \sum_{k=1}^n a_{k-1} \varphi_{k-1}(u) \quad \text{and} \quad B_u^n(a) = \sum_{k=n+1}^{\infty} a_{k-1} \varphi_{k-1}(u);$$

as the n -th order partial sum in (4) and the corresponding "tail" series, respectively. In terms of these sums, the Brownian bridge is expressed as $B_u^0(a) = S_u^n(a) + B_u^n(a)$. Obviously, B_u^n and S_u^n are independent. Moreover, a standard theorem regarding the sum of independent Gaussian distributed random variables shows that B_u^n and S_u^n are again Gaussian distributed random variables of mean zero and variances

$$E(B_u^n)^2 = \sum_{k=n+1}^{\infty} \varphi_{k-1}^2(u) \quad \text{and} \quad E(S_u^n)^2 = \sum_{k=1}^n \varphi_{k-1}^2(u);$$

respectively. By independence, we have the equality

$$E(B_u^0)^2 = E(B_u^n)^2 + E(S_u^n)^2 = u(1-u); \quad (9)$$

where we used the fact that the variance of the Brownian bridge does not depend upon the series representation and so, it can be computed by using any convenient basis (e.g. the sine-Fourier basis).

A natural way of measuring the quality of the approximation $S_u^n(a)$ to $B_u^0(a)$ is the value of the time average of the variances of the tails

$$\int_0^1 E(B_u^0 - S_u^n)^2 du = \int_0^1 E(B_u^n)^2 du = \int_0^1 \sum_{k=1}^n \varphi_{k-1}^2(u) du; \quad (10)$$

Intuitively, the best approximating series is the one that minimizes the functional (10) for each n (we shall show that the answer is indeed a series). More clearly, we want to find $f_{k-1}(u)$; $k \geq 1$; such that the system of functions on the interval $[0;1]$ which, together with the constant function $\varphi_0(u) = 1$, make up an orthonormal system in $L^2[0;1]$ and which realizes the maximum of the functional

$$G(1; \dots; n) = \int_0^1 \sum_{k=1}^n f_{k-1}^2(u) du; \quad (11)$$

Since the system $\sqrt{2} \cos(k\pi u) g_{k-1}$ together with the constant function make up a complete orthonormal system of $L^2[0;1]$, we may write

$$f_{k-1}(u) = \sqrt{2} \cos(k\pi u) \int_0^1 f_{k-1}(v) \sqrt{2} \cos(k\pi v) dv;$$

Replacing this in (11), we obtain

$$G(1; \dots; n) = \int_0^1 \sum_{k=1}^n f_{k-1}^2(u) du = \int_0^1 \sum_{k=1}^n \sum_{l=1}^{\infty} \sum_{j=1}^{\infty} \varphi_{k-1}(u) \varphi_{l-1}(u) \cos(l\pi u) \cos(j\pi u) du = \int_0^1 \sum_{k=1}^n \sum_{l=1}^{\infty} \varphi_{k-1}(u) \varphi_{l-1}(u) \frac{2 \cos(l\pi u) \cos(l\pi u)}{l^2} du; \quad (12)$$

where we used the fact that the system $\sqrt{2} \sin(k\pi u) g_{k-1}$ is also orthonormal. From the theory of integral equations with symmetric kernels, we learn that the maximum of (12) is realized on the set of the n eigenfunctions having the largest eigenvalues. Since the kernel is already in the series representation form, the maximum of our problem is $\sum_{k=1}^n \frac{1}{k^2}$ and is attained on the (orthonormal) functions

$$f_{k-1}(u) = \sqrt{2} \cos(k\pi u) \quad k \geq 1; n:$$

It follows that the Wiener representation is the unique series for which the time-average of the variance of the

tail series reaches the minimum value of

$$\int_0^1 E(B_u^0 - S_u^n)^2 du = \frac{1}{6} \sum_{k=1}^n \frac{1}{k^2}; \quad (13)$$

However, there is a direct connection between the asymptotic rate of convergence of the primitive method and the quantity $E(B_u^0 - S_u^n)^2$, a connection that is given by formula (20) and is analyzed in Section IIIA. It allows us to conclude that the Wiener representation is the best series for general use in the primitive method.

III. IMPROVEMENTS IN THE PRIMITIVE FOURIER PATH INTEGRAL TECHNIQUE

In the primitive series approach [c.f. Eq. (8)], the "tail" portion of the Brownian bridge is simply discarded. Rather than neglecting these terms entirely, it is possible to include (approximately) their effects through a number of approaches. One of these is known as the partial averaging method.⁹ Another is a method we term the reweighted method introduced in Section IIIB. We note that in both methods the n -th order partial sum S_u^n is unchanged, its distribution being identical to the primitive method one. All methods which preserve the distribution of the partial sum S_u^n are referred to by the name of the respective series. As such, if the sine-Fourier basis is

utilized, we shall call the aforementioned approaches the PA-FPI and the RW-FPI methods, respectively.

A. Partial Averaging Method

Developed initially for the Fourier path integral method, the partial averaging technique can be defined for all series representations. The key is the independence of the coordinates a_k , which physically amounts to choosing those representations for which the kinetic energy operator is diagonal. Denoting by E_n the average over the coefficients beyond the rank n , the partial averaging formula reads:

$$\frac{Z_{PA}^n(x; x^0; \beta)}{Z_{FP}^n(x; x^0; \beta)} = \int_R d(a_1) \cdots \int_R d(a_n) \exp$$

$$E_n \int_0^{\beta} \frac{1}{V} x_0(u) + \frac{S}{m_0} \sum_{k=1}^{\infty} \frac{X^k}{a_k} x_k(u) du \quad (14)$$

As we mentioned before, the series $\sum_{k=n+1}^{\infty} a_k x_k(u)$ is again a Gaussian distributed variable of mean zero and variance $E(S_u^n)^2$. Using this together with the equal-

ity (9), it is not difficult to show that formula (14) becomes

$$\frac{Z_{PA}^n(x; x^0; \beta)}{Z_{FP}^n(x; x^0; \beta)} = \int_R d(a_1) \cdots \int_R d(a_n) \exp$$

$$\int_0^{\beta} \frac{1}{V_{u,n}} x_0(u) + \frac{S}{m_0} \sum_{k=1}^{\infty} \frac{X^k}{a_k} x_k(u) du ; \quad (15)$$

where

$$\frac{1}{V_{u,n}}(x) = \int_R \frac{1}{2^{n/2} (u)} \exp \left[-\frac{z^2}{2^{n/2} (u)} \right] V(x+z) dz; \quad (16)$$

with $2_n(u)$ defined by

$$2_n(u) = \frac{1}{m_0} \sum_{k=1}^{\infty} u(1-u) X_k^n x_k(u)^2 ; \quad (17)$$

There is one property of the partial averaging method of particular note: an application of Jensen's inequality¹² shows that

$$\begin{aligned} \frac{Z_{PA}^{n+1}(x; x^0; \beta)}{Z_{FP}^{n+1}(x; x^0; \beta)} &= \int_R d(a_1) \cdots \int_R d(a_n) \int_R d(a_{n+1}) \exp \\ &\quad \int_0^{\beta} \frac{1}{V} x_0(u) + \frac{S}{m_0} \sum_{k=1}^{\infty} \frac{X^k}{a_k} x_k(u) du \\ &\quad \int_R d(a_1) \cdots \int_R d(a_n) \exp \\ &\quad \int_0^{\beta} \frac{1}{V_{u,n}} x_0(u) + \frac{S}{m_0} \sum_{k=1}^{\infty} \frac{X^k}{a_k} x_k(u) du = (18) \\ &\quad \int_R d(a_1) \cdots \int_R d(a_n) \exp \\ &\quad \int_0^{\beta} \frac{1}{V_{u,n}} x_0(u) + \frac{S}{m_0} \sum_{k=1}^{\infty} \frac{X^k}{a_k} x_k(u) du = \frac{Z_{PA}^n(x; x^0; \beta)}{Z_{FP}^n(x; x^0; \beta)} ; \end{aligned}$$

Therefore, the sequence

$$\rho_{PA}^0(x; x^0;) \quad \rho_{PA}^1(x; x^0;) \quad \dots \quad \rho_{PA}^n(x; x^0;) \quad \dots \quad (19)$$

is an increasing sequence that converges from below to the true density matrix, $\rho(x; x^0;)$.

Let us now consider the problem of choosing the best series representation for use within the partial averaging framework. We notice that the sequence $\rho_n^2(u)$, given by formula (17), decreases monotonically while $\rho_{PA}^n(x; x^0;)$ increases monotonically, as shown by formula (19). In fact, there is a connection between (17) and (19) in the sense that the faster the Gaussian spread converges to zero, the faster $\bar{V}_{u,n}(x)$ converges to the original potential $V(x)$, and the faster $\rho_{PA}^n(x; x^0;)$ increases to

$\rho(x; x^0;)$. We note that this observation is general, independent of the potential $V(x)$. Of course, one may try to optimize $\rho_{PA}^n(x; x^0;)$ directly, but then the best basis will depend upon the potential, an undesirable computational feature. We thus conclude that the optimal basis for the partial averaging method is the one for which the time-average of $\rho_n^2(u)$ has the fastest decrease to zero, i.e. the Wiener or Fourier basis. In this sense, the best partial averaging method is the PA-FPI approach.

We now present one final argument in favor of the Wiener basis, an argument that will lead us to a new computational approach, the reweighted FPI technique. Remembering the primitive random series method (8) and defining

$$X_1(x; x^0; a;) = \exp \left\{ \int_0^h V(x_0(u) + \frac{1}{m_0} \sum_{k=1}^n a_k \cdot \frac{1}{\sqrt{2}} X_k^i(u)) du \right\};$$

and

$$X_n(x; x^0; a;) = \exp \left\{ \int_0^h V(x_0(u) + \frac{1}{m_0} \sum_{k=1}^n a_k \cdot \frac{1}{\sqrt{2}} X_k^i(u)) du \right\};$$

respectively, we have to the first-order in :

$$\begin{aligned} E_n X_1(x; x^0; a;) &= \int_0^h \int \left(V(x_0(u) + \frac{1}{m_0} \sum_{k=1}^n a_k \cdot \frac{1}{\sqrt{2}} X_k^i(u)) \right) \bar{V}_{u,n}(x_0(u) + \frac{1}{m_0} \sum_{k=1}^n a_k \cdot \frac{1}{\sqrt{2}} X_k^i(u)) du \\ &= \int_0^h \int \left(V(x_0(u) + \frac{1}{m_0} \sum_{k=1}^n a_k \cdot \frac{1}{\sqrt{2}} X_k^i(u)) \right) \rho_n^2(u) du \end{aligned} \quad (20)$$

The rate of convergence for the primitive random series method thus depends on the difference between $V(x)$ and $\bar{V}_{u,n}(x)$, which in turn depends on the value of $\rho_n^2(u)$. Therefore, to a first approximation, the differences between the exact and the n -th order FPI density matrices depend not on the detailed structure of the respective tails, but rather on the spread of the tail series, $B_u^n(a)$, a quantity whose time average reaches a minimum for the Wiener series. One can readily verify that the term of order ϵ^2 vanishes for the partial averaging analog of formula (20), an indication that the technique exactly accounts for the extra spread of the paths induced by the tail series.

B. Reweighting Method

Unlike the partial averaging method, the reweighting technique attempts to account for the effects of the tail series in a way that does not involve modifying the associated potential energy. We shall work out the result

for the Wiener basis, noting that: (1) the approach can be applied to any arbitrary representation, and (2) the efficiency of the method will depend upon the specific series selected. The basic idea is to replace $B_u^n(a)$ by another collection, $R_u^n(b_1; \dots, b_n)$, which is supported by an n -dimensional underlying probability space. We require that:

1. The variance at the point u of $R_u^n(b_1; \dots, b_n)$, denoted by $\sigma_n^2(u)$, be as close as possible to $\rho_n^2(u)$.
2. The variables $S_u^n(a_1; \dots, a_n)$ and $R_u^n(b_1; \dots, b_n)$ be independent and their sum have a joint distribution as close to a Brownian bridge as possible.

One possible candidate for our approach is to choose $R_u^n(b_1; \dots, b_n) = \frac{1}{m_0} \sum_{k=1}^n b_k \cdot \frac{1}{\sqrt{2}} X_k^i(u)$; with $b_1; \dots, b_n$ independent identically distributed standard normal random variables. Condition 2 above is realized in the Ito-Nisio theorem by insuring that the collection $\{ \cos(k u); 1 \leq k \leq \infty \}$ is orthogonal, where $X_k(u)$ is the

derivative of $\chi_k(u)$. We shall enforce this condition by choosing $\chi_k(u) = \sum_{j=1}^n \alpha_{n,jk} \sin[(k+jn)u]$ where $\alpha_{n,jk}$ are some constants yet to be determined. With the condition 1 above in mind, and by noticing that in the exact FPI representation (7) the terms of the form $\sin[(k+jn)u]$ with $j \geq 1$ "decouple" as $n \rightarrow \infty$, our intuition tells us that a good candidate for $\alpha_{n,jk}$ is

$$\alpha_{n,jk} = \frac{2}{\pi} \sum_{j=1}^n \frac{1}{(k+jn)^2}.$$

With this choice, the n -th order RW-FPI density matrix is given by the formula

$$\frac{\rho_{RW}^n(x; x^0; \beta)}{\rho_P(x; x^0; \beta)} = \int_{-\infty}^{\infty} dP[a] \exp \left(\sum_{k=1}^n \int_0^1 du \sum_{j=1}^n \alpha_{n,jk} \sin(ku) \right) \quad (21)$$

where

$$\alpha_{n,jk} = \frac{2}{\pi} \sum_{j=1}^n \frac{1}{(k+jn)^2} \quad \begin{cases} < 1/k^2; & \text{if } 1 \leq k \leq n \\ > 1/(k+n)^2; & \text{if } n < k \leq 2n \end{cases} \quad (22)$$

The evaluation of the path weights $\alpha_{n,jk}$ is discussed in Appendix D.

Clearly, our choice of $\rho_u^n(x; x^0; \beta)$ is not unique. For a better understanding of the quality of the approximation, let us compare numerically:

$\rho_n^2(u)$, the tail variance for the full FPI representation and for the PA-FPI method,

$\rho_n^2(u) = \sum_{k=n+1}^{2n} \sum_{j=1}^n \alpha_{n,jk} \sin(ku)^2$, the tail variance for the RW-FPI method, and

$\rho_n^2(u) = \sum_{k=n+1}^{2n} \frac{2}{k} \sin(ku)^2$, the tail variance for the FPI method if it were computed without reweighting (i.e. by simply considering the next n Fourier terms).

Fig 1 plots the above variances for $n = 9$. We notice that $\rho_n^2(u)$ and $\rho_n^2(u)$ are indeed close, much closer than the result obtained by simply expanding the primitive FPI approach with a similar number of additional terms.

IV. ASYMPTOTIC CONVERGENCE OF THE FPI TECHNIQUES

We say that a given method converges asymptotically as $O(1/n)$ if the partition function, the density matrix

at each pair of points $(x; x^0)$, and their first-order temperature derivatives converge as fast as $O(1/n)$. Generally speaking, the aforementioned quantities may have different asymptotic rates of convergence. However, if the potential is smooth enough, our intuition says that this

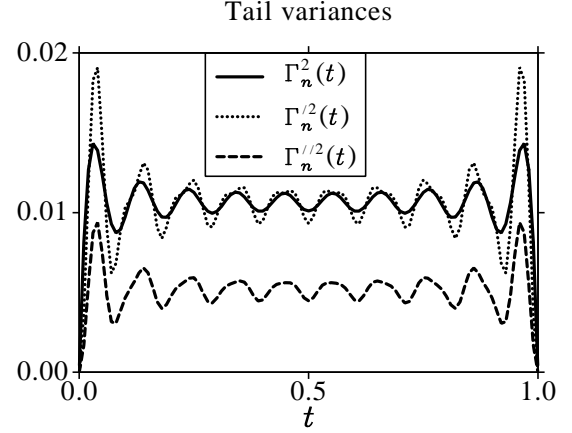


FIG. 1: A plot of the tail variances for the PA-FPI, RW-FPI, and $2n$ -order primitive FPI for $n = 9$. Notice that the simple inclusion of the next 9 terms within the primitive FPI is not the optimal strategy.

is not true. For the case of the harmonic oscillator, we shall only verify the convergence of the partition function. On the other hand, for numerical simulations it is more convenient to compute the average energy of the system with the help of the so called T-estimator, which can solely be expressed as a functional of the diagonal density matrix:

$$\langle E \rangle^T = \frac{\partial}{\partial \beta} \ln \int_{\mathcal{R}} \rho(x; \beta) dx \quad (23)$$

The above formula can be expressed as the statistical average

$$\langle E \rangle^T = \frac{\int_{\mathcal{R}} dx \int_{\mathcal{R}} dP[a] \chi_n(x; a; \beta) E_n^T(x; a; \beta)}{\int_{\mathcal{R}} dx \int_{\mathcal{R}} dP[a] \chi_n(x; a; \beta)}; \quad (24)$$

which can be evaluated by Monte Carlo integration. Using the notation

$$\chi_n(a; u; \beta) = \sum_{k=1}^{2n} \alpha_{n,k} \sin(ku)$$

to denote the stochastic portions of the current path truncated to the first n terms, one easily deduces that the T-estimator function for the primitive FPI method is

$$E_n^T(\mathbf{x}; \mathbf{a};) = \frac{1}{2} + \int_0^{Z-1} V[\mathbf{x} + \mathbf{x}_n(\mathbf{a}; u;)] du + \frac{1}{2} \int_0^{Z-1} V^0[\mathbf{x} + \mathbf{x}_n(\mathbf{a}; u;)] \mathbf{x}_n(\mathbf{a}; u;) du; \quad (25)$$

while for the PA-FPI method, one obtains

$$E_n^T(\mathbf{x}; \mathbf{a};) = \frac{1}{2} + \int_0^{Z-1} \frac{1}{V_{u,n}} [\mathbf{x} + \mathbf{x}_n(\mathbf{a}; u;)] du + \frac{1}{2} \int_0^{Z-1} \frac{1}{V_{u,n}^0} [\mathbf{x} + \mathbf{x}_n(\mathbf{a}; u;)] \mathbf{x}_n(\mathbf{a}; u;) du + \frac{1}{2} \int_0^{Z-1} \frac{1}{V_{u,n}^0} [\mathbf{x} + \mathbf{x}_n(\mathbf{a}; u;)] \frac{d^2}{du^2} (u) du; \quad (26)$$

By a simple integration by parts against the coordinate \mathbf{x} , one may eliminate the second derivative of the potential and obtain the following equivalent PA-FPI energy estimator:

$$E_n^T(\mathbf{x}; \mathbf{a};) = \frac{1}{2} + \int_0^{Z-1} \frac{1}{V_{u,n}} [\mathbf{x} + \mathbf{x}_n(\mathbf{a}; u;)] du + \frac{1}{2} \int_0^{Z-1} \frac{1}{V_{u,n}^0} [\mathbf{x} + \mathbf{x}_n(\mathbf{a}; u;)] \mathbf{x}_n(\mathbf{a}; u;) du + \frac{1}{2} \int_0^{Z-1} \frac{1}{V_{u,n}^0} [\mathbf{x} + \mathbf{x}_n(\mathbf{a}; u;)] \frac{d^2}{du^2} (u) du - \frac{1}{2} \int_0^{Z-1} \frac{1}{V_{u,n}^0} [\mathbf{x} + \mathbf{x}_n(\mathbf{a}; u;)] du; \quad (27)$$

The T-estimator for the RW-FPI method has the same expression as the one for primitive FPI, except for the redefinition of the current path

$$\mathbf{x}_n(\mathbf{a}; u;) = \sum_{k=1}^{X^n} a_{k-n;k} \sin(k u);$$

It is important to note that because of the way we have included the temperature dependence of the path distribution in the above analysis, we have obtained directly the so called "virial" forms of the energy estimators. These virial expressions have desirable variance properties^{10,13} and are generally preferred for precise Monte Carlo applications. The special form (27) of the PA-FPI energy estimator is numerically advantageous since it does not require the evaluation of the second derivatives of the averaged potential. Although we do not study it in this paper because it is not a functional of the diagonal density matrix, the H-estimator for the PA-FPI method can similarly be put in the simple form:

$$E_n^H(\mathbf{x}; \mathbf{a};) = \frac{1}{2} + V(\mathbf{x}) + \frac{\hbar^2}{4m_0} \int_0^{Z-1} \int_0^{Z-1} \frac{1}{V_{u,n}} [\mathbf{x} + \mathbf{x}_n(\mathbf{a}; u;)] \frac{d^2}{du^2} (u) \frac{1}{V_{v,n}^0} [\mathbf{x} + \mathbf{x}_n(\mathbf{a}; v;)] du dv; \quad (28)$$

The equivalent H-estimator functions for the primitive FPI and RW-FPI approaches look formally the same, except that the potential is no longer averaged. The H-estimator is thus properly defined even for potentials that do not have second-order derivatives. The reader should notice that the double integral appearing in (28) is really a sum of products of monodimensional integrals. We chose this representation for symmetry purposes. The estimator is thus the sum of the "classical" energy and a "quantum" correction term.

A. Partition functions for the harmonic oscillator

In Ref. 10, enough analytical evidence was presented to suggest that the asymptotic behavior of the primitive and partial averaging FPI methods is controlled at most by the values of the second derivatives of the potential. Here, we conjecture that this remains true of the RW-FPI method, so that an analysis of the harmonic oscillator, the simplest potential having a non-vanishing second-order derivative, should provide a reliable guess of the asymptotic rates for all "smooth" potentials (defined here as the potentials having continuous second-order derivatives). Therefore, we shall study the asymptotic conver-

gence of the partition function for a one-dimensional particle of mass $m_0 = 1$ moving in the quadratic potential $V(\mathbf{x}) = \mathbf{x}^2/2$. We also set $\hbar = 1$ and $\beta = 1$.

The exact analytical expressions for the harmonic oscillator partition functions are derived in the Appendix B for the three methods: primitive FPI, PA-FPI, and RW-FPI, respectively. The partition functions of even and odd orders have a slightly different convergence behavior according to whether $1 - (1/\beta)$ is 0 or 2 (see Appendix B). To avoid the appearance of certain oscillations in our plots, we shall only compute the odd subsequence for the RW-FPI method. Remember, however, that the $2n + 1$ -th order RW-FPI approach uses in fact twice as many points. To ensure fairness as far as the computational

error is concerned, we shall compare the $2n + 1$ -th order RW-FPI results with those of the $4n + 2$ -th order primitive FPI and PA-FPI approaches since, for a given order, the former method uses twice as many path variables as do the latter techniques. It is convenient to redefine the order of the RW-FPI method as being equal to the number of random variables used to parameterize the paths, in this case: $4n + 2$. In general,

$$\frac{Z_{RW}^{2n}(x; x^0; \beta)}{Z_{FP}(x; x^0; \beta)} = \int \mathcal{D}[\mathbf{a}] \exp \left[-\int_0^1 V(x_0(u) + \sum_{k=1}^{2n} a_{k-1,k} \sin(ku)) du \right]; \quad (29)$$

where $a_{n,k}$ is given by formula (22) and is evaluated in Appendix D.

Let us assume that we may expand the difference $Z_{Pr}^n(\beta) - Z(\beta)$ as the generalized power series

$$Z_{Pr}^n(\beta) - Z(\beta) = \frac{c}{n} + \sum_{k=1}^{\infty} \frac{\alpha_k}{n^k};$$

with $c \neq 0$. For n large enough, it suffices to consider the approximation

$$Z_{Pr}^n(\beta) - Z(\beta) \approx \frac{c}{n} + \frac{c_1}{n}; \quad (30)$$

By passing to the subsequence $4n + 2$ and taking the ratios of consecutive differences, we obtain:

$$\frac{Z_{Pr}^{4n+2}(\beta) - Z(\beta)}{Z_{Pr}^{4n+2}(\beta) - Z(\beta)} = \frac{4n+2}{4n-2} \frac{1 + c_1/(4n+2)}{1 + c_1/(4n-2)};$$

Next, we take the logarithm and use the approximation $\log(1+x) \approx x$ for the last term:

$$\log \left[1 + \frac{Z_{Pr}^{4n+2}(\beta) - Z(\beta)}{Z_{Pr}^{4n+2}(\beta) - Z(\beta)} \right] = \log \left[1 + \frac{4}{4n-2} + \log \left[1 + \frac{c_1}{4n^2-1} \right] \right];$$

We expand the logarithms on the right-hand side of the above equation so that the error be of the order $O(1/n^3)$ and then multiply the resulting equation by $n^2 - 1 = 4$ to obtain

$$(n^2 - 1 = 4) \log \left[1 + \frac{Z_{Pr}^{4n+2}(\beta) - Z(\beta)}{Z_{Pr}^{4n+2}(\beta) - Z(\beta)} \right] = n + \frac{4n+2}{4n-2} + \frac{c_1}{4n^2-1}; \quad q=4;$$

It is convenient to introduce the notation

$$D Z_{Pr}^{4n+2}(\beta) = Z_{Pr}^{4n+2}(\beta) - Z_{Pr}^{4n+2}(\beta)$$

and set

$$n_{Pr} = (n^2 - 1 = 4) \log \left[1 + \frac{D Z_{Pr}^{4n+2}(\beta)}{Z_{Pr}^{4n+2}(\beta) - Z(\beta)} \right];$$

Asymptotic rate for the quadratic potential

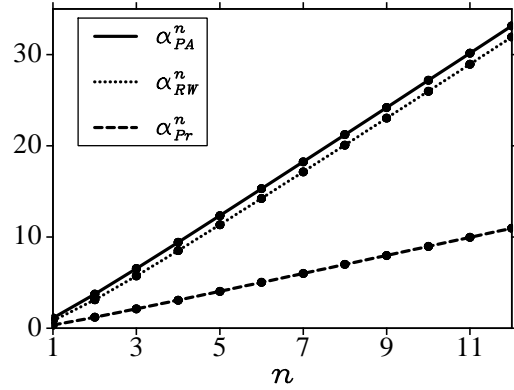


FIG. 2: A plot of the indices of convergence for the PA-FPI, RW-FPI, and primitive FPI for the quadratic potential.

Since $(4n + 2) = (4n - 2) + 4$ for n large, we conclude

$$n_{Pr} \approx n + 2 \frac{c_1}{4}; \quad (31)$$

which shows that n_{Pr} should be asymptotically a straight line whose slope gives the convergence order. Here, $Z(\beta)$ is the exact value of the partition function and the index Pr is used to denote the primitive FPI method. Of course, similar expressions can be written for the other two methods identified by the indices RW and PA . For general expressions which apply to any of the techniques, we shall use the index Mt .

Once the asymptotic order is established, we may determine the value of the constant c by analyzing the slope of the equation

$$c_{Mt}^n = c n + c = 2 + c q; \quad (32)$$

where

$$c_{Mt}^n = (4n + 2) (n + 1 = 2) \frac{Z_{Mt}^{4n+2}(\beta) - Z(\beta)}{Z_{Mt}^{4n+2}(\beta) - Z(\beta)};$$

The asymptotic behavior implied by (32) can easily be established by replacing n by $4n + 2$ in equation (30).

Fig. 2 shows that the linear region predicted by our analysis is quite rapidly reached for the harmonic oscillator. One easily notices that the PA-FPI and RW-FPI methods have similar asymptotic behavior, while the primitive FPI approach has a slower rate of convergence.

The asymptotic slopes are computed as the slope of the line that best fits the last $[N=3]$ values, where N is the number of data points calculated. We assume that we computed enough points so that the last $[N=3]$ are in the asymptotic region. Euler least-square fit gives then the value

$$M_t = \frac{[N=3] \sum_{k=1}^N k^k c_{Mt}^k}{[N=3] \sum_{k=1}^N k^k}; \quad (33)$$

where the summation is done over the last $[N=3]$ data points. Of course, the exact value for is the limit as $N \rightarrow 1$ of the right-hand side of the above formula. For $N = 12$, (33) gives: $c_{PR} = 1.002$, $c_{PA} = 3.007$ and $c_{RW} = 3.008$, suggesting that the asymptotic behavior is $O(1/n)$ for the first, and $O(1/n^3)$ for the last two methods, respectively.

The constants c are calculated in a similar fashion and the numerical values for $N = 12$ are: $c_{PR} = 0.049$, $c_{PA} = 7.933 \cdot 10^{-3}$, and $c_{RW} = 0.887$, respectively. Therefore, the partial averaging method is superior to the reweighted method in the sense that it has a smaller convergence constant (smaller in modulus).

Theoretically, if we can compute the difference between successive values of the partition function with sufficient precision, we can improve the convergence of any of the FPI methods by using better estimators. For first-order, the result can be obtained as follows: formula (30) shows that

$$Z_{Mt}^{4n+2}(\cdot) = \frac{c}{(4n+2)} \quad (34)$$

converges to the exact answer as fast as $O(1/(4n+2)^{+1})$ and therefore, the last equation is a better estimator as far as the asymptotic behavior is concerned. Given that the convergence exponent is known, the constant c can be approximately (but arbitrarily exactly as $n \rightarrow 1$) evaluated from the equation:

$$D Z_{Mt}^{4n+2}(\cdot) = \frac{(4n+2)}{(4n+2)} \frac{(4n-2)}{(4n-2)} = \frac{c}{(4n+2)n}$$

Solving for c and replacing in (34), one ends up with the first-order corrected estimator

$$F Z_{Mt}^{4n+2}(\cdot) = Z_{Mt}^{4n+2}(\cdot) - \frac{n}{4n+2} D Z_{Mt}^{4n+2}(\cdot) \quad (35)$$

The second-order estimator can be derived by applying the first-order correction to the first-order estimator. One easily computes:

$$\begin{aligned} S Z_{Mt}^{4n+2}(\cdot) = Z_{Mt}^{4n+2}(\cdot) & - \frac{(2+1)n}{(4+1)} D Z_{Mt}^{4n+2}(\cdot) \\ & - \frac{n}{(4+1)} D Z_{Mt}^{4n+2}(\cdot) + \\ & + \frac{n^2}{(4+1)} D^2 Z_{Mt}^{4n+2}(\cdot) - D Z_{Mt}^{4n+2}(\cdot) \end{aligned} \quad (36)$$

The asymptotic convergence of this estimator is $O(1/n^{+2})$.

In principle, one can continue this process beyond second-order. However, as we shall see in the Appendix E, such higher order estimators are of little practical value. To demonstrate the behavior of the corrected estimators, we compute the convergence exponents for the primitive FPI using the corresponding analog of equation (31). Fig. 3 clearly shows the difference in the rate of convergence for the original and corrected estimators.

Asymptotic rates for different estimators

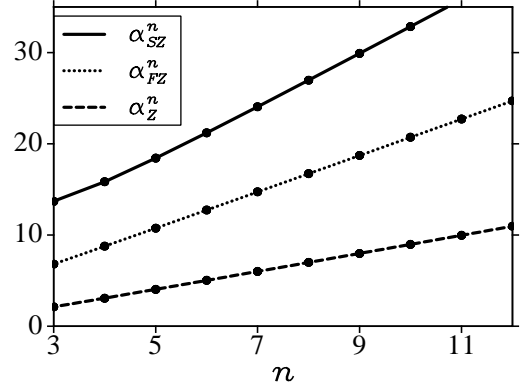


FIG. 3: A plot of the exponents of convergence for the three Z-estimators. The method employed is primitive FPI as applied to the quadratic potential.

The numerical values are $c_Z = 1.002$, $c_{FZ} = 1.997$, and $c_{SZ} = 2.958$, demonstrating our predictions. From now on, we shall refer to the original, unaccelerated estimator as the zero-order estimator.

B. A numerical example: The quartic potential

As we said in the beginning of this section, for numerical purposes it is convenient to study the convergence of the T-method energy estimator in the virial form, which can be computed by Monte Carlo integration. As we explain below, the numerical study of the asymptotic behavior is not a computationally easy task, especially for those methods that have rapid asymptotic convergence. More explicitly, let us take a look at the following analog of (31):

$$\frac{n}{M_t} = \frac{E_{Mt}^{4n+2}}{E_{Mt}^{4n+2}} - \frac{E_{Mt}^{4n+2}}{E_{Mt}^{4n+2}}; \quad (37)$$

where

$$\frac{n}{M_t} = (n^2 - 1) \log 1 + \frac{E_{Mt}^{4n+2}}{E_{Mt}^{4n+2}} - \frac{E_{Mt}^{4n+2}}{E_{Mt}^{4n+2}} :$$

For the partial averaging method, we suggested that the difference $E_{PA}^{4n+2} - E$ decays to zero as fast as $1/n^3$. In turn, the differences $E_{PA}^{4n+2} - E_{PA}^{4n+2}$ between consecutive terms decay to zero as fast as $1/n^4$. It is thus clear that faster rates of convergence of the method require greater precision in the evaluation of the terms E_{PA}^{4n+2} . If we assume an independent sampling of the probability density shown in formula (24), the error in the Monte Carlo evaluation of E_{PA}^{4n+2} is $E_{PA}^{4n+2} = \frac{E_{PA}^{4n+2}}{\sqrt{N}}$, where N is the number of Monte Carlo sampling points and E_{PA}^{4n+2} is the standard deviation. This error should satisfy the

inequality:

$$j E_{PA}^{4n+2} \leq \frac{E_{PA}^{4n+2}}{E_{PA}^{4n+2}} \leq E_{PA}^{4n+2} j$$

It follows that the number of Monte Carlo points necessary to insure a given relative error for E_{PA} scales at least as badly as $N \propto n^8$ as a function of the number of Fourier coefficients. The same is true for RW-FPI, while for the primitive FPI we only need $N \propto n^4$. We emphasize that this scaling is related to our immediate task of establishing the asymptotic rates of convergence and is not an issue that would arise in typical numerical applications.

The second observation we make is that the ratio

$$\frac{E_{Mt}^{4n+2}}{E_{Mt}^{4n+2}} \leq \frac{E_{Mt}^{4n+2}}{E_{Mt}^{4n+2}} \leq \frac{E_{Mt}^{4n+2}}{E_{Mt}^{4n+2}}$$

increases as the temperature is dropped. Consequently, we would like to conduct our model computations at low temperature, where the quantum effects are big enough so that the differences between consecutive terms are significant. At high temperature, the classical limit is a good approximation and these differences may be smaller than the statistical errors we are able to achieve. We are therefore forced to conduct our computations in the "unfavorable" range of temperatures, and in general, we need to study groundstate problems.

We hope this is enough rationale to justify the need for a special Monte Carlo integration scheme capable of accurately sampling the low temperature distributions with good efficiency and low correlation, at least for certain classes of simpler systems. One such scheme is discussed in Appendix E, and it generally applies to the class of single-well potentials.

For comparison purposes, we shall also compute the T-estimator energies for the trapezoidal Trotter method. Expressions similar to those presented here for the FPI methods were deduced by Coalson¹⁴ and employed by Mielke and Tnuhlar² as the TT-FPI method. We shall keep this name in the present paper, though, as defined here, the TT-FPI approach is not an FPI method because the n -th order partial sum S_u^n is not the one for the primitive FPI. The importance of this method consists of the fact that its asymptotic rate of convergence is $O(1/n^2)$ for smooth enough potentials, being the fastest primitive method to date that leaves the potential unchanged.¹⁵ We do not present this scheme in the present paper and for further information we refer the reader to the cited literature.

The prototype system studied in this work is the quartic potential $V(x) = x^4/2$. We set $\hbar = 1$ and $m_0 = 1$ and $\beta = 10$. The groundstate of the quartic potential was evaluated by variational methods to be $E_0 = 0.530181$, while the average energy at the temperature corresponding to $\beta = 10$ is $E = 0.530183$. We computed the average energy for the sequence $4n+2$ with $1 \leq n \leq 12$, corresponding to the actual numbers of Fourier coefficients 6;10;14;18;22;26;30;34;38;42;46;50. In these calculations, the number of points employed in the Gauss-Legendre quadrature scheme was

Asymptotic rate for the quartic potential

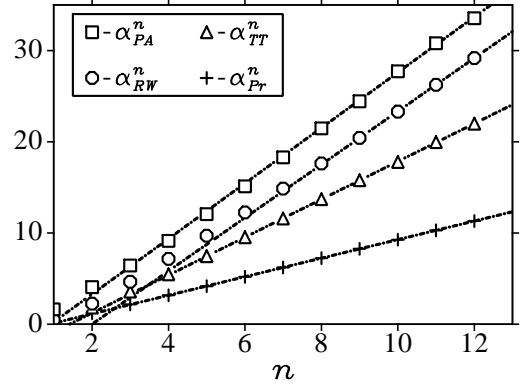


FIG. 4: The straight lines drawn represent the linear least square fit for the last four data. Their slopes give the convergence exponents for each method.

200. We used 125 10 Monte Carlo points for primitive FPI, 25 10 for TT-FPI, 5 10 points for RW-FPI, and 2 10 points for PA-FPI calculations, respectively. The values of R_{PA}^{4n+2} were previously computed in a quarter of these numbers during a "warm-up" period, but we continued to improve them during the main Monte Carlo procedure. Table I of Appendix F summarizes the results of the computer evaluations. The differences between successive energy terms were computed with the help of the estimator (E9). The errors were computed with the help of the formulae (E3) for the average energies, and (E11) for the estimated differences.

Fig 4 shows the behavior of the functions $\frac{n}{M_t}$ for the four methods. Among the non-averaged methods, we remark that the primitive FPI approach reaches its asymptotic behavior faster than the TT-FPI method, which in turn reaches its asymptotic region faster than the RW-FPI technique. This behavior is shown in Fig 5, which plots the current slope $\frac{n}{M_t} - \frac{n-1}{M_t-1}$. Although the RW-FPI method did not reach its final asymptotic behavior, the trend is clear. The computed convergence exponents using the last four data points are: $\alpha_{PA} = 3.082$, $\alpha_{RW} = 2.917$, $\alpha_{TT} = 2.071$, and $\alpha_{Pr} = 1.019$. Therefore, we conclude that the asymptotic convergence of the methods is $O(1/n^3)$ for PA-FPI and RW-FPI, $O(1/n^2)$ for TT-FPI, and $O(1/n)$ for primitive FPI. Lastly, it is worth comparing the convergence constants for the PA-FPI and RW-FPI methods since they have the same asymptotic convergence exponent. The numerical values are $C_{PA} = 59.4$ and $C_{RW} = 736.7$, showing that the PA-FPI method is over 10 times faster than the RW-FPI method. This is in agreement with the observations made for the partition function of the harmonic oscillator in the previous section. The PA speed-up of the convergence is important, especially with respect to minimizing the number of path variables required in practical applications.

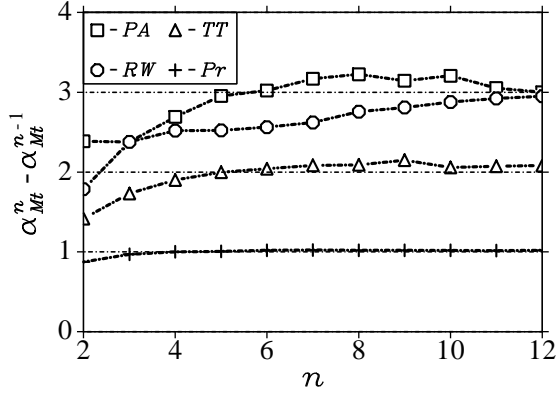


FIG. 5: The current slopes for each method should ideally converge to 3 for PA-FPI and RW-FPI, 2 for TT-FPI, and 1 for primitive FPI.

V. CONCLUSIONS

In this paper, we have shown that the best series representation (with respect to asymptotic convergence) for use in Monte Carlo path integral methods is the Wiener sine-Fourier series. Both the RW-FPI and TT-FPI methods are not series representations and we suggest that the latter also falls in the category of reweighting techniques. The partial averaging technique has the asymptotic convergence $O(1/n^3)$, with a small convergence constant and

it is the best way of improving the asymptotic behavior of the primitive FPI method (at the cost of computing the Gaussian transform of the potential). The TT-FPI and RW-FPI methods increase the order of convergence of the primitive FPI to $O(1/n^2)$, and $O(1/n^3)$, respectively, without increasing the variance of the corresponding estimators. It should be noted that, unlike the complete partial averaging approach, the reweighting method does not require the Gaussian transform of the potential. While a final decision awaits detailed future studies, we anticipate that this latter feature of the reweighting approach will be beneficial for applications where the Gaussian transform is either formally ill-posed and/or computationally difficult to obtain. Finally, as discussed in Appendix E, the first and the second-order estimators also improve the asymptotic convergence. Although both have larger variances, the first order estimator appears computationally feasible since its variance decreases with the number of Fourier coefficients.

Acknowledgments

The authors acknowledge support from the National Science Foundation through awards CDA-9724347, CHE-0095053, and CHE-0131114. They also would like to thank Professor D. L. Freeman and Dr. Dubravko Sabo for continuing discussions concerning the present developments.

- ¹ D. M. Ceperley, Rev. Mod. Phys. 67, 279 (1995).
- ² S. L. Mielke and D. G. Truhlar, J. Chem. Phys. 114, 621 (2001).
- ³ R. P. Feynman, Rev. Modern Phys. 20, 367 (1948).
- ⁴ M. Kac, in Proceedings of the 2nd Berkeley Symposium on Mathematical Statistics and Probability (University of California, Berkeley, 1951) pp. 189-215.
- ⁵ R. Durrett, Probability: Theory and Examples, 2nd ed. (Duxbury, New York, 1996), pp. 430-431.
- ⁶ B. Simon, Functional Integration and Quantum Physics (Academic, London, 1979).
- ⁷ S. Kwapień and W. A. Woyczyński, Random Series and Stochastic Integrals: Single and Multiple (Birkhauser, Boston, 1992), Chap. 2.5.
- ⁸ J. D. Doll and D. L. Freeman, J. Chem. Phys. 80, 2239 (1984).
- ⁹ J. D. Doll, R. D. Coalson, and D. L. Freeman, Phys. Rev. Lett. 55, 1 (1985).
- ¹⁰ M. Eleftheriou, J. D. Doll, E. Curotto, and D. L. Freeman, J. Chem. Phys. 110, 6657 (1998).
- ¹¹ N. Wiener, J. of Math. and Phys. 2, 131 (1923).
- ¹² See Probability: Theory and Examples (Ref. 5), p. 14.
- ¹³ D. L. Freeman and J. D. Doll, J. Chem. Phys. 80, 5709 (1984).
- ¹⁴ R. D. Coalson, J. Chem. Phys. 85, 926 (1986).
- ¹⁵ H. De Raedt and B. De Raedt, Phys. Rev. A 28, 3575

- (1983).
- ¹⁶ N. Metropolis, A. W. Rosenbluth, M. N. Rosenbluth, A. M. Teller, and E. Teller J. Chem. Phys. 21, 1087 (1953).
- ¹⁷ M. Kalos and P. Whitlock, Monte Carlo Methods (Wiley-Interscience, New York, 1986).
- ¹⁸ W. Feller, An Introduction to Probability Theory and its Applications (John Wiley and Sons, New York, 1950), Vol. 1, p. 324.
- ¹⁹ D. Sabo, D. L. Freeman, and J. D. Doll, J. Chem. Phys. 113, 2522 (2000).

APPENDIX A: ITO-NISIO THEOREM

Theorem 1 (Ito-Nisio⁷) Let $\{f_k(\cdot)g_{k,0}\}$ be any orthonormal basis in $L^2[0;1]$ such that $f_0(\cdot) = 1$, let

$$Z_u = \sum_{k=1}^{\infty} \int_0^1 f_k(u) g_{k,0}(u) du;$$

and let $\{a_k g_{k,1}\}$ be a sequence of independent identically distributed (i.i.d.) standard normal random variables. Then, the series

$$\sum_{k=1}^{\infty} a_k \int_0^1 f_k(u) g_{k,1}(u) du$$

APPENDIX B: HARMONIC OSCILLATOR

The $2n$ -th order primitive FPI approximation of the partition function for an harmonic oscillator centered at the origin has the expression

$$Z_{Pr}^{2n}(\cdot) = \int_{\mathbb{R}} dx \int_{\mathbb{R}} da_1 \dots \int_{\mathbb{R}} da_{2n} \int_{\mathbb{R}} \mathcal{P}_n(x; a; \cdot);$$

where

$$\mathcal{P}_n(x; a; \cdot) = \left(\frac{m_0}{2} \right)^n \exp \left(-\frac{1}{2} \sum_{k=1}^{2n} a_k^2 \right) \exp \left(\frac{m_0!}{2} \sum_{k=1}^{2n} a_k \sin(ku) \right) du;$$

By explicitly computing the integral over t and then completing the square, one obtains

$$\mathcal{P}_n(x; a; \cdot) = \left(\frac{m_0}{2} \right)^n \exp \left(-\frac{1}{2} \sum_{k=1}^{2n} a_k^2 \right) \exp \left(\frac{m_0!}{2} \sum_{k=1}^{2n} a_k \sin(ku) \right) du; \quad (B1)$$

where

$$\frac{m_0!}{2} = 1 + \frac{m_0!}{2} \sum_{k=1}^{2n} a_k^2;$$

For use as a trial density in Monte Carlo simulations, it is convenient to replace the last factor by its limit $n \rightarrow \infty$:

$$\mathcal{P}_{tr}^{2n}(x; a; \cdot) = \left(\frac{m_0}{2} \right)^n \exp \left(-\frac{1}{2} \sum_{k=1}^{2n} a_k^2 \right) \exp \left(\frac{m_0!}{2} \sum_{k=1}^{2n} a_k \sin(ku) \right) du; \quad (B2)$$

It is not difficult to show that the trial densities for the primitive FPI and PA-FPI methods are identical (after normalization) but we shall employ formula (B2) for the RW-FPI technique too. Practice shows that the penalty for considering the last two approximations is minimal, while (B2) has some advantages with regard to the organization of the computations.

To evaluate the partition functions for the primitive FPI approach, we integrate (B1) and obtain

$$Z_{Pr}^{2n}(\cdot) = \frac{1}{n!} \int_{\mathbb{R}} \prod_{k=1}^{2n} da_k \int_{\mathbb{R}} dx \left(\frac{m_0!}{2} \sum_{k=1}^{2n} a_k \sin(ku) \right)^{n-1}; \quad (B3)$$

We leave for the reader the simple task of showing that the $2n$ -th order PA-FPI density matrix has the form

$$Z_{PA}^{2n}(\cdot) = Z_{Pr}^{2n}(\cdot) \exp \left(-\frac{1}{2} \sum_{k=1}^{2n} a_k^2 \right) \exp \left(\frac{m_0!}{2} \sum_{k=1}^{2n} a_k \sin(ku) \right); \quad (B4)$$

where \mathbf{x}^0 has the standard normal distribution and

$$r_1(f) = \frac{\int_0^1 f(x) dx}{\int_0^1 f(x^0) dx} = 1 + 2 \sum_{n=1}^{\infty} r_n(f) : \quad (C5)$$

If the sampling were independent, the correlation coefficients would vanish and we would recover the classical central limit theorem. In practice however, the correlation coefficients are positive, many times having a slow decay to zero and the independent sampling may be considered a fortunate case. Without entering the details, we mention that there are two factors that contribute to large correlation coefficients: a) a strongly correlated pro-

posals $T(\mathbf{x}^0|\mathbf{x})$ and b) a low overall efficiency. The overall efficiency (or the acceptance ratio) is defined as

$$Ac = \frac{\int \mathbf{x}^0 d\mathbf{x}^0}{\int \mathbf{x} d\mathbf{x}} \frac{A(\mathbf{x}^0|\mathbf{x})T(\mathbf{x}^0|\mathbf{x})}{A(\mathbf{x}|\mathbf{x}^0)} \quad (C6)$$

and represents the fraction of moves accepted. Therefore, if the overall efficiency has large enough values ($Ac \geq 0.2$), it is a good idea to use an independent proposal from a trial probability $\text{tr}(\mathbf{x})$. If $\text{tr}(\mathbf{x}) \approx \mathbf{x}$ and $f(\mathbf{x})$ is smooth enough, we may approximately relate the correlation coefficients to the overall efficiency as follows: from the relation (C1), we easily compute

$$r_1(f) = 1 - \frac{\int \mathbf{x}^0 d\mathbf{x}^0 \int \mathbf{x} d\mathbf{x} [f(\mathbf{x})^2 - f(\mathbf{x})f(\mathbf{x}^0)]}{\int \mathbf{x}^0 d\mathbf{x}^0 \int \mathbf{x} d\mathbf{x} [f(\mathbf{x})^2 - f(\mathbf{x})f(\mathbf{x}^0)]} \frac{\text{tr}(\mathbf{x})A(\mathbf{x}^0|\mathbf{x})}{A(\mathbf{x}|\mathbf{x}^0)};$$

where

$$A(\mathbf{x}^0|\mathbf{x}) = \min_{\mathbf{x}^0} \left[1; \frac{\text{tr}(\mathbf{x})}{A(\mathbf{x}|\mathbf{x}^0)} \right] : \quad (C7)$$

Using the approximation $\text{tr}(\mathbf{x})A(\mathbf{x}^0|\mathbf{x}) \approx A(\mathbf{x}|\mathbf{x}^0)$, the right-hand side simplifies to $r_1(f) \approx 1 - Ac$. In general, by a similar line of thought, one may argue that $r_n(f) \approx (1 - Ac)^n$. The formula (C5) takes the approximate value

$$r_1(f) \approx \frac{\int_0^1 f(x) dx}{\int_0^1 f(x^0) dx} = 1 + 2 \sum_{n=1}^{\infty} (1 - Ac)^n = \frac{2}{Ac} - 1 : \quad (C8)$$

Therefore, the bigger the acceptance probability, the faster the convergence of the Monte Carlo procedure. In the limit $Ac = 1$, we recover the independent sampling, but a quick look at formula (C7) shows that in this case $\text{tr}(\mathbf{x}) = \mathbf{x}$.

APPENDIX D: COMPUTATION OF THE PATH WEIGHTS $w_{n,k}$ FOR THE RW-FPIMETHOD.

If $n < k - 2n$, we have

$$w_{n,k} = \frac{2^{-2} \sum_{j=0}^k \frac{1}{(k-jn)^2}}{2^{m_0} n^2} = \frac{2^{-2} \sum_{j=0}^k \frac{1}{(k-jn)^2}}{2^{m_0} n^2} h\left(\frac{k-n}{n}\right); \quad (D1)$$

where

$$h(x) = \sum_{j=1}^{\infty} \frac{1}{(j+x)^2} :$$

Clearly, the values of the function $h(x)$ are only needed over the interval $[0;1]$ and they can be evaluated via the

Hurwitz ζ -function, usually implemented by many mathematical libraries. Alternatively, $h(x)$ can be evaluated via the trivial identity

$$h(x) = \sum_{j=1}^{\infty} \frac{1}{(j+x)^2} = \frac{1}{x^2} \sum_{j=1}^{\infty} \frac{1}{(1+\frac{j}{x})^2} = \frac{1}{x^2} \sum_{j=1}^{\infty} \frac{1}{(1+\frac{j}{x})^2} ; \quad (D2)$$

where $\zeta(s)$ is the Riemann ζ -function

$$\zeta(s) = \sum_{n=1}^{\infty} \frac{1}{n^s} :$$

We have $\zeta(2) = \frac{\pi^2}{6}$, $\zeta(3) = 1.2020569031596$, and $\zeta(4) = \frac{\pi^4}{90}$, with the last series in (D2) converging quite fast. More precisely, the error in the evaluation of $h(x)$ committed by truncating the series to the first n terms is easily seen to be smaller than $\sum_{j>n}^{\infty} \frac{1}{j^4} = \frac{1}{n^3}$ uniformly on the whole interval $[0;1]$, so that summation over the first 100 terms gives the value of $h(x)$ with an error of at most 10^{-8} . This error is sufficiently small for our applications.

APPENDIX E: A SPECIALIZED MONTE CARLO SCHEME

As suggested in Appendix C, the use of an independent trial distribution in the Metropolis algorithm is a good strategy provided that we are able to find a good approximation $\text{tr}^{4n+2}(\mathbf{x}; a; \cdot)$ to the density we need to sample in this case,

$$\text{tr}^{4n+2}(\mathbf{x}; a; \cdot) = \frac{X_{M \pm}^{4n+2}(\mathbf{x}; a; \cdot)}{(2)^{2n+1}} \exp \left[-\frac{1}{2} \sum_{k=1}^n a_k^2 \right] : \quad (E1)$$

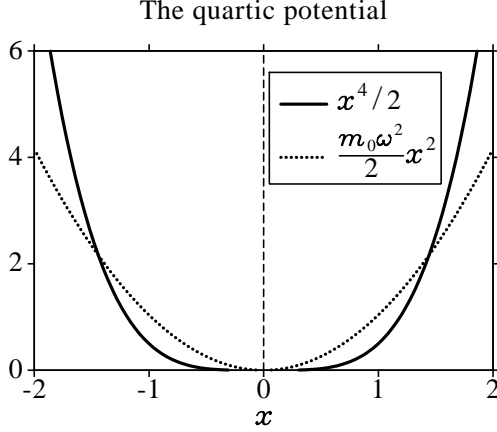


FIG. 6: A plot of the quartic potential (solid line) and its best variational quadratic approximation. Here, $m_0 = 1$ and $\omega = 1.442$.

This approximation may be taken to be the similar expression for a harmonic oscillator potential $m_0 \omega^2 (x - A)^2/2$, because we know how to generate an independent sample of this. In order for the approximation to work well for many of the single well potentials of interest, we optimize the parameters ω and A to obtain a best fit in the sense of increasing the overall acceptance ratio. However, since we are analyzing groundstate problems, sufficiently good approximations can be obtained from the Ritz variational principle. Thus, we look for the parameters ω and A which realize the minimum of the functional

$$E(\omega; A) = \int_{-\infty}^{\infty} \psi_A^\dagger \hat{H} \psi_A dx;$$

where

$$\psi_A(x) = \frac{m_0 \omega^{1/4}}{\sqrt{2\pi}} \exp\left(-\frac{m_0 \omega^2}{2} (x - A)^2\right)$$

is the groundstate eigenfunction of the trial harmonic potential and

$$\hat{H} = \frac{\hbar^2}{2m_0} \frac{d^2}{dx^2} + V(x)$$

is the Hamiltonian of the original single well potential. By a translation of the reference system, we may assume that the optimizing parameter A is zero. For the case of the quartic potential $V(x) = x^4/2$, the best optimizing parameters are $\omega = 1.442$ and $A = 0$. Fig. 6 plots the quartic potential and its best quadratic approximation.

Rather than using the $4n+2$ -th order probability density of the best harmonic reference as the trial density, it is more convenient to use the slightly modified formula (B2) of Appendix B. The advantage is that (B2) is the exponential of a series. As such, if we generate the vector $(x; a_0; \dots; a_{4n+2})$ from the probability density $\rho_{4n+2}^{tr}(x; a; \omega)$ given by (B2), we can use the vectors of the

form $(x; a_0; \dots; a_{4k+2})$ with $k \leq n$ for the paths of smaller length because it is clear that these vectors are drawn from the distribution $\rho_{4k+2}^{tr}(x; a; \omega)$. The time saved with the generation of random numbers fully compensates the slight decrease in the acceptance ratio. We use (B2) for all FPI methods in the following examples.

For PA-FPI and primitive FPI, there is another advantage in using the trial density (B2). A large portion of the computational time is spent with the construction of the paths

$$a_{4n+2}(u; \omega) = \sum_{k=1}^{4n+2} a_k \sin(ku);$$

especially for large n . However, if the trial probability density (B2) is used, we can employ the recurrence formula

$$a_{4n+2}(u; \omega) = a_{4n-2}(u; \omega) + \sum_{k=4n-1}^{4n+2} a_k \sin(ku);$$

Therefore, the time necessary to construct all the paths of length $4k+2$ with $1 \leq k \leq n$ at a given point t scales like $O(n)$ instead of $O(n^2)$. This is especially important for the PA-FPI method, which has the fastest convergence and for which a large number of Monte Carlo steps is necessary to establish the asymptotic convergence rate. Unfortunately, since the paths for RW-FPI are not series, we cannot employ the same strategy for this method.

As shown in the Appendix C, the advantage of our Monte Carlo strategy consists of the fact that it has low correlation provided that the acceptance ratio is large. To a first approximation, the statistical error in the estimation of the energy is [we employ the usual definition for the error, corresponding to a confidence interval of 95.4%]

$$Err_s(E_{Mt}^{4n+2}) = \frac{2 \sigma_0^2 E_{Mt}^{4n+2}}{N} \frac{1}{Ac} \quad (E2)$$

where N is the number of Monte Carlo points, $\sigma_0^2 E_{Mt}^{4n+2}$ is the variance of the T-estimator function, and Ac is the acceptance ratio [see (C8)]. A more precise formula is given by (C5):

$$Err_s(E_{Mt}^{4n+2}) = \frac{2 \sigma_0^2 E_{Mt}^{4n+2}}{N} \left(1 + 2 \sum_{k=1}^n r_k E_{Mt}^{4n+2} \right) \quad (E3)$$

and we have shown in Appendix C how the correlation coefficients can be evaluated during the Monte Carlo procedure. However, we can use (E2) to find the number of steps after which the correlation becomes negligible. In the case of the quartic potential, the acceptance ratio was bigger than 0.6 for all simulations performed. Since $2 \sigma_0^2 E_{Mt}^{4n+2} = 2.333 \dots + 2 \sum_{k=1}^8 0.4^k = 2.332$, we may safely truncate the series in (E3) to the first eight correlation coefficients and we shall do so for all computations concerning the quartic potential.

Another important aspect in our computations is the numerical evaluation of the one-dimensional time averages that are involved. This issue was extensively studied by Sabo et. al.,¹⁹ who concluded that a Gauss-Legendre quadrature in a number of points equal to three times the number of Fourier coefficients should suffice for most applications. We also employ the Gauss-Legendre quadrature scheme, but in a number of points equal to four times the maximum number of Fourier coefficients computed. Extensive computer observations show that the relative error in the evaluation of the T-estimator func-

tion is smaller than 10^{-8} for the quartic potential. Of course, for real-life applications we do not need such a precision but here it is important to rule out any factor likely to alter the asymptotic law of convergence.

Earlier in this section, we saw that the scaling of the number of Monte Carlo points with the number of Fourier coefficients was dictated by the decay of the differences $E_{M,t}^{4n-2} - E_{M,t}^{4n+2}$, which we shall denote by $DE_{M,t}^{4n+2}$. We shall improve on this fact by directly evaluating these differences with the help of a biased estimator. Define

$$r_{M,t}^{4n+2}(x;a_j) = X_{M,t}^{4n-2}(x;a_j) - X_{M,t}^{4n+2}(x;a_j) \quad (E4)$$

and

$$R_{M,t}^{4n+2} = \frac{\int_{-R}^R dx \int_{-R}^R dP \int_{-R}^R dX_{4n+2}(x;a_j) r_{M,t}^{4n+2}(x;a_j)}{\int_{-R}^R dx \int_{-R}^R dP \int_{-R}^R dX_{4n+2}(x;a_j)} : \quad (E5)$$

Next, define

$$DE_{4n+2}^{T,M,t}(x;a_j) = E_{4n-2}^{T,M,t}(x;a_j) - r_{M,t}^{4n+2}(x;a_j) = R_{M,t}^{4n+2} - E_{4n+2}^{T,M,t}(x;a_j) : \quad (E6)$$

It is a simple exercise to show that

$$E_{M,t}^{4n-2} - E_{M,t}^{4n+2} = \frac{\int_{-R}^R dx \int_{-R}^R dP \int_{-R}^R dX_{4n+2}(x;a_j) DE_{4n+2}^{T,M,t}(x;a_j)}{\int_{-R}^R dx \int_{-R}^R dP \int_{-R}^R dX_{4n+2}(x;a_j)} : \quad (E7)$$

A biased estimator for the function (E6) can be constructed as follows: assume you are given a sequence $(x_k; a_k)$ with $1 \leq k \leq N$, which samples the probability distribution (E1). At step k , compute

$$R_{M,t}^{k;4n+2} = \frac{1}{k} \sum_{j=1}^k r_{M,t}^{4n+2}(x_j; a_j) \quad \text{and} \quad Err_s(k; R_{M,t}^{4n+2}) :$$

and construct the function

$$DE_{k;4n+2}^{T,M,t}(x;a_j) = E_{4n-2}^{T,M,t}(x;a_j) - r_{M,t}^{k;4n+2}(x;a_j) = R_{M,t}^{k;4n+2} - E_{4n+2}^{T,M,t}(x;a_j) : \quad (E8)$$

Then, the biased estimator is defined by the well-known recurrence formula

$$DE_{M,t}^{k;4n+2} = (k-1)DE_{M,t}^{k-1;4n+2} + DE_{k;4n+2}^{T,M,t}(x_k; a_k) \quad (E9)$$

starting with $DE_{M,t}^{0;4n+2} = 0$. Clearly, $DE_{M,t}^{k;4n+2}$ converges to $DE_{M,t}^{4n+2}$ as k gets large.

The bias in (E8) is due to the fact that we do not use the exact value of $R_{M,t}^{4n+2}$ but its unbiased statistical estimator. However, for large enough k , it is not difficult to justify the estimate:

$$DE_{k;4n+2}^{T,M,t}(x;a_j) - DE_{4n+2}^{T,M,t}(x;a_j) \sim \frac{E_{4n-2}^{T,M,t}(x;a_j) - R_{M,t}^{4n+2}(x;a_j)}{R_{M,t}^{4n+2}} \frac{Err_s(k; R_{M,t}^{4n+2})}{R_{M,t}^{4n+2}} :$$

It follows then that the error due to bias is at most

$$Err_b(N; DE_{M,t}^{4n+2}) = \frac{1}{N} \sum_{k=1}^N \frac{E_{4n-2}^{T,M,t}(x_k; a_k) - R_{M,t}^{4n+2}(x_k; a_k)}{R_{M,t}^{k;4n+2}} \frac{Err_s(k; R_{M,t}^{4n+2})}{R_{M,t}^{k;4n+2}} : \quad (E10)$$

The total error is then obtained by also adding the statistical error computed with the help of the formula (E3):

$$Err(N; DE_{M,t}^{4n+2}) = Err_s(N; DE_{M,t}^{4n+2}) + Err_b(N; DE_{M,t}^{4n+2}) : \quad (E11)$$

In the present paper, we pre-computed a start value of $R_{M,t}^{4n+2}$ using a quarter of the number of Monte Carlo points during the warm-up step and then continued to improve the value in the main procedure. In these conditions, one may argue that the error for the difference (E 7) satisfies the inequality

$$\text{Err}(N; D E_{M,t}^{4n+2}) = \text{Err}_s(N; D E_{M,t}^{4n+2}) + \frac{P}{5} E_{M,t}^{4n+2} \frac{\text{Err}_s(5N=4; R_{M,t}^{4n+2})}{R_{M,t}^{4n+2}}; \quad (\text{E } 12)$$

where

$$E_{M,t}^{4n+2} = \frac{\int_{\mathcal{R}} dx \int_{\mathcal{R}} d\mathbf{p} \int_{\mathcal{R}} d\mathbf{X} X_{4n+2}(\mathbf{x}; \mathbf{a};) E_{4n+2}^{T,M,t}(\mathbf{x}; \mathbf{a};)}{\int_{\mathcal{R}} dx \int_{\mathcal{R}} d\mathbf{p} \int_{\mathcal{R}} d\mathbf{X} X_{4n+2}(\mathbf{x}; \mathbf{a};)};$$

Formula (E 12) helps us explain why the use of the biased estimator (E 8) is advantageous. Had we directly evaluated the difference

$$D E_{M,t}^{4n+2} = E_{M,t}^{4n+2} - E_{M,t}^{4n+2}; \quad (\text{E } 13)$$

the error would have been

$$\text{Err}(N; D E_{M,t}^{4n+2}) = \text{Err}_s(N; E_{M,t}^{4n+2}) + \text{Err}_s(N; E_{M,t}^{4n+2}); \quad (\text{E } 14)$$

Notice however that both $r_{M,t}^{4n+2}(\mathbf{x}; \mathbf{a};)$ and $D E_{4n+2}^{T,M,t}(\mathbf{x}; \mathbf{a};)$ converge to 1 and 0, respectively as $n \rightarrow 1$. In turn, their variances (which control the statistical errors) converge to zero. Clearly, this is not the case for the variance of the T-method energy estimator. More precisely, Table II presents strong numerical evidence suggesting that the decay of their standard deviations is as fast as $O(1/n^2)$ and we expect this to be true for all smooth enough potentials. This implies that for a fixed but large number of Monte Carlo points N , the error in (E 11) has the asymptotic behavior

$$\text{Err}(N; D E_{4n+2}^{T,M,t}) \sim \frac{\text{const}}{n^2 N} \quad (\text{E } 15)$$

The importance of (E 15) is twofold. First, it shows that if the estimator (E 9) is used, the scaling of the number of Monte Carlo samples with respect to the number of Fourier coefficients is now determined by the decay of $E_{M,t}^{4n+2}$ to zero. More precisely, we have $N \propto n^6$ for PA-FPI and RW-FPI, $N \propto n^4$ for TT-FPI, and $N \propto n^2$ for primitive FPI.

Second, the errors of the estimators of order one and two [see (35) and (36)] have the asymptotic behavior:

$$\begin{aligned} \text{Err}(N; E_{4n+2}^{T,M,t}) &= \text{Err}_s(N; E_{4n+2}^{T,M,t}) + \frac{1}{n} \frac{\text{const}}{N} \\ &\quad \text{Err}(N; E_{4n+2}^{T,M,t}) \end{aligned} \quad (\text{E } 16)$$

and,

$$\begin{aligned} \text{Err}(N; S E_{4n+2}^{T,M,t}) &= \text{Err}_s(N; E_{4n+2}^{T,M,t}) + \\ &\quad \frac{\text{const}}{(n+1)N} \left(\frac{2}{n} + \frac{1}{n-1} + 2 + \frac{2n^2}{(n-1)^2} \right) \\ &\quad \text{Err}_s(N; E_{4n+2}^{T,M,t}) + \frac{4}{(n+1)N} \frac{\text{const}}{N} \end{aligned} \quad (\text{E } 17)$$

This readily implies that the use of the estimators of order one and two does not change the scaling of the number of Monte Carlo points needed to achieve a given error threshold for the estimated energy with the number of Fourier coefficients. The net result is an improvement in the asymptotic behavior for the estimators of order one and two. However, in the case of the second-order estimator, we notice an increase in the variance of the estimator which may be quite large for practical purposes. For the first-order estimator there is no asymptotic increase in the variance, which makes it more suitable for practical applications. In fact, the first-order estimator may also be used for potentials that do not have continuous second-order derivatives but for which the decay with the number of Fourier coefficients implied by (E 15) can be replaced by the slower one

$$\text{Err}(N; D E_{4n+2}^{T,M,t}) \sim \frac{\text{const}}{n N};$$

Finally, in the cases where it cannot be utilized as an energy estimator because of an unduly large variance, the correction term brought in by the first-order estimator is still useful as a measure of how far the zero-order estimator is from the true result.

The reader may work out the expression for the estimator of order three and see that in this case the scaling is changed. This explains our earlier assertion that the estimators of order three or more are of little practical value.

APPENDIX F: TABLES OF NUMERICAL VALUES

The following tables contain the numerical results described in Section IV B. See that discussion for the details.

TABLE I: Average energies, estimated differences, and their statistical error for the quartic potential at $\alpha = 10$. The variational energy is 0.530183.

| n | 1 | 2 | 3 | 4 | 5 | 6 | 7 | 8 | 9 | 10 | 11 | 12 |
|---|----------|----------|----------|----------|----------|----------|----------|----------|----------|----------|----------|----------|
| Average energies | | | | | | | | | | | | |
| $E_{P_r}^{4n+2}$ | 0.302878 | 0.365234 | 0.401528 | 0.425003 | 0.441342 | 0.453379 | 0.462581 | 0.469834 | 0.475704 | 0.480548 | 0.484613 | 0.488071 |
| $E_{T_T}^{4n+2}$ | 0.343731 | 0.416263 | 0.454541 | 0.476808 | 0.490728 | 0.499978 | 0.506376 | 0.510972 | 0.514391 | 0.516994 | 0.518994 | 0.520602 |
| $E_{R_W}^{4n+2}$ | 0.351676 | 0.432846 | 0.473011 | 0.493918 | 0.505667 | 0.512786 | 0.517363 | 0.520451 | 0.522627 | 0.524201 | 0.525370 | 0.526247 |
| $E_{P_A}^{4n+2}$ | 0.596947 | 0.552843 | 0.541042 | 0.536268 | 0.533916 | 0.532629 | 0.531862 | 0.531383 | 0.531069 | 0.530854 | 0.530701 | 0.530593 |
| Estimated differences | | | | | | | | | | | | |
| $D E_{P_r}^{4n+2}$ | -124981 | -062354 | -036316 | -023475 | -016353 | -012025 | -009205 | -007265 | -005872 | -004848 | -004062 | -003452 |
| $D E_{T_T}^{4n+2}$ | -147346 | -072843 | -038307 | -022241 | -013929 | -009222 | -006401 | -0046052 | -003424 | -002593 | -002013 | -001589 |
| $D E_{R_W}^{4n+2}$ | -162238 | -080976 | -040075 | -020896 | -011746 | -007111 | -004573 | -003100 | -002176 | -001575 | -001168 | -000886 |
| $D E_{P_A}^{4n+2}$ | 0.549021 | 0.044095 | 0.011781 | 0.004772 | 0.002347 | 0.001285 | 0.000763 | 0.000481 | 0.000316 | 0.000216 | 0.000151 | 0.000109 |
| Statistical errors for energies (2) | | | | | | | | | | | | |
| $E_{P_r}^{4n+2}$ | 0.000088 | 0.000084 | 0.000081 | 0.000080 | 0.000078 | 0.000078 | 0.000077 | 0.000077 | 0.000076 | 0.000076 | 0.000076 | 0.000076 |
| $E_{T_T}^{4n+2}$ | 0.000056 | 0.000057 | 0.000056 | 0.000055 | 0.000054 | 0.000054 | 0.000054 | 0.000053 | 0.000053 | 0.000053 | 0.000053 | 0.000053 |
| $E_{R_W}^{4n+2}$ | 0.000043 | 0.000042 | 0.000041 | 0.000040 | 0.000039 | 0.000038 | 0.000038 | 0.000038 | 0.000038 | 0.000037 | 0.000037 | 0.000037 |
| $E_{P_A}^{4n+2}$ | 0.000024 | 0.000023 | 0.000021 | 0.000020 | 0.000020 | 0.000020 | 0.000020 | 0.000019 | 0.000019 | 0.000019 | 0.000018 | 0.000018 |
| Statistical errors for differences (2) | | | | | | | | | | | | |
| $D E_{P_r}^{4n+2}$ | 0.032356 | 0.000304 | 0.000095 | 0.000055 | 0.000036 | 0.000026 | 0.000020 | 0.000016 | 0.000012 | 0.000010 | 0.000009 | 0.000007 |
| $D E_{T_T}^{4n+2}$ | 0.054577 | 0.001325 | 0.000199 | 0.000092 | 0.000061 | 0.000046 | 0.000036 | 0.000030 | 0.000025 | 0.000021 | 0.000018 | 0.000015 |
| $D E_{R_W}^{4n+2}$ | 0.037799 | 0.001600 | 0.000333 | 0.000074 | 0.000045 | 0.000032 | 0.000025 | 0.000019 | 0.000016 | 0.000013 | 0.000011 | 0.000009 |
| $D E_{P_A}^{4n+2}$ | 0.004595 | 0.000080 | 0.000027 | 0.000014 | 0.000009 | 0.000007 | 0.000005 | 0.000004 | 0.000003 | 0.000003 | 0.000002 | 0.000002 |

TABLE II: Standard deviations for $r_{M_t}^{4n+2}(x;a)$ and $D E_{4n+1}^{T;M_t}(x;a)$ and their asymptotic convergence exponents α .

| n | 2 | 3 | 4 | 5 | 6 | 7 | 8 | 9 | 10 | 11 | 12 | |
|----------------------|----------|----------|----------|----------|----------|----------|----------|----------|----------|----------|----------|-------|
| Primitive FPI | | | | | | | | | | | | |
| $r_{P_r}^{4n+2}$ | 1.771976 | 0.437892 | 0.226571 | 0.143267 | 0.099735 | 0.073744 | 0.056769 | 0.045052 | 0.036617 | 0.030341 | 0.025542 | 2.027 |
| $D E_{4n+2}^{T;P_r}$ | 0.907676 | 0.222962 | 0.116896 | 0.075168 | 0.052794 | 0.039381 | 0.030502 | 0.024296 | 0.019827 | 0.016464 | 0.013907 | 1.985 |
| TT-FPI | | | | | | | | | | | | |
| $r_{T_T}^{4n+2}$ | 9.411364 | 1.149898 | 0.499554 | 0.326273 | 0.241282 | 0.187604 | 0.151356 | 0.125104 | 0.105345 | 0.090015 | 0.077867 | 1.822 |
| $D E_{4n+2}^{T;T_T}$ | 5.259389 | 0.856299 | 0.342638 | 0.204763 | 0.148354 | 0.112764 | 0.089384 | 0.072996 | 0.060898 | 0.051628 | 0.044358 | 1.825 |
| RW-FPI | | | | | | | | | | | | |
| $r_{R_W}^{4n+2}$ | 17.63636 | 1.953891 | 0.543819 | 0.324225 | 0.228415 | 0.171841 | 0.134647 | 0.108553 | 0.089442 | 0.074985 | 0.063776 | 1.961 |
| $D E_{4n+2}^{T;R_W}$ | 8.421340 | 2.378073 | 0.393884 | 0.210005 | 0.142382 | 0.105825 | 0.082139 | 0.065720 | 0.053826 | 0.044884 | 0.037983 | 1.999 |
| PA-FPI | | | | | | | | | | | | |
| $r_{P_A}^{4n+2}$ | 1.164360 | 0.309710 | 0.182490 | 0.122904 | 0.088704 | 0.067010 | 0.052355 | 0.041982 | 0.034380 | 0.028648 | 0.024221 | 2.100 |
| $D E_{4n+2}^{T;P_A}$ | 1.596240 | 0.291506 | 0.142120 | 0.087909 | 0.060274 | 0.044039 | 0.033599 | 0.026465 | 0.021387 | 0.017629 | 0.014785 | 2.013 |